

# NIHAO XI: Formation of Ultra-Diffuse Galaxies by outflows

Arianna Di Cintio<sup>1\*</sup>, Chris B. Brook<sup>2</sup>, Aaron A. Dutton<sup>3</sup>, Andrea V. Macciò<sup>3,4</sup>,  
 Aura Obreja<sup>3</sup> & Avishai Dekel<sup>5</sup>

<sup>1</sup>Dark-Carlsberg Fellow, Dark Cosmology Centre, NBI, University of Copenhagen, Juliane Maries Vej 30, DK-2100 Copenhagen, Denmark

<sup>2</sup>Ramon y Cajal Fellow, Universidad de La Laguna and Instituto de Astrofísica de Canarias, E-38206, La Laguna, Tenerife, Spain

<sup>3</sup>New York University Abu Dhabi, PO Box 129188, Abu Dhabi, United Arab Emirates

<sup>4</sup>Max Planck Institute für Astronomie, Königstuhl 17, 69117 Heidelberg, Germany

<sup>5</sup>Center for Astrophysics and Planetary Science, Racah Institute of Physics, The Hebrew University, Jerusalem 91904, Israel

Accepted xxxx. Received xxxx; in original form xxxx

## ABSTRACT

We address the origin of Ultra-Diffuse Galaxies (UDGs), which have stellar masses typical of dwarf galaxies but effective radii of Milky Way-sized objects. Their formation mechanism, and whether they are failed  $L_*$  galaxies or diffuse dwarfs, are challenging issues. Using zoom-in cosmological simulations from the NIHAO project, we show that UDG analogues form naturally in dwarf-sized haloes due to episodes of gas outflows associated with star formation. The simulated UDGs live in isolated haloes of masses  $10^{10-11}M_\odot$ , have stellar masses of  $10^{7-8.5}M_\odot$ , effective radii larger than 1 kpc and dark matter cores. They show a broad range of colors, an average Sérsic index of 0.83, a typical distribution of halo spin and concentration, and a non-negligible HI gas mass of  $10^{7-9}M_\odot$ , which correlates with the extent of the galaxy. Gas availability is crucial to the internal processes that form UDGs: feedback driven gas outflows, and subsequent dark matter and stellar expansion, are the key to reproduce faint, yet unusually extended, galaxies. This scenario implies that UDGs represent a dwarf population of low surface brightness galaxies and should exist in the field. The largest isolated UDGs should contain more HI gas than less extended dwarfs of similar  $M^*$ .

**Key words:** galaxies: dwarf - evolution - formation - haloes

## 1 INTRODUCTION

Deep imaging of nearby clusters have revealed a sizeable population of faint,  $M_R \gtrsim -16.5$ , low surface brightness,  $\mu_e = 24-28$  mag/arcsec<sup>2</sup>, and unusually large,  $0.8 < r_e / \text{kpc} < 5$  galaxies, named Ultra-Diffuse Galaxies or UDGs (van Dokkum et al. 2015a). While their stellar masses are typical of dwarfs,  $10^7 < M^* / M_\odot < 10^{8.7}$ , their effective radii are compatible with  $L_*$  objects, raising doubts about the nature of such galaxies. Almost 1000 UDGs have been identified in the Coma cluster using the Dragonfly array (van Dokkum et al. 2015a,b) and the Subaru telescope (Koda et al. 2015; Yagi et al. 2016): they represent a passively evolving population, lying on the red sequence in the color-magnitude diagram, as opposed to classical low surface brightness (LSB) galaxies which are bluer and brighter (e.g. McGaugh et al. 1995; Impey & Bothun 1997; Schombert et al. 2011). Red UDGs have since been found in the Virgo cluster (Mihos et al. 2015), with even lower SB than the Virgo LSBs discovered 30 years ago by Sandage & Binggeli (1984). Confirming the existence of an abundant population of such objects, UDGs have also been observed in Fornax and other clusters (Muñoz et al. 2015; van der Burg et al. 2016). However, UDGs

may not necessarily be red and associated with clusters: Roman & Trujillo (2016) studied a region around the Abell 168 cluster, showing that about half of its UDGs are found outside the main cluster overdensity, with their properties changing towards the cluster centre, suggestive of environmental effects; they also observed bluer UDGs than in Coma. Corroborating the idea that UDGs can form in isolation, Martínez-Delgado et al. (2016) found a UDG in the outskirts of the Pisces-Perseus supercluster, DGSAT I, that shows a blue over-density compatible with recent star formation.

While some authors envision a scenario in which UDGs are failed  $L_*$  galaxies that lost their gas after forming the first stars (van Dokkum et al. 2015a,b), some others argue that they are genuine dwarf galaxies possibly living in high-spin haloes (Amorisco & Loeb 2016). Supporting the first claim are simulations by Yozin & Bekki (2015), indicating that UDGs may be underdeveloped galaxies whose early accretion onto a cluster quenched further growth. Favouring a massive halo for UDGs is the inferred virial mass of  $\sim 8 \times 10^{11}M_\odot$  for DF 44<sup>1</sup>, one of the brightest Coma UDGs (van Dokkum et al. 2016). This result is in contrast with the derived mass of two other UDGs: using the abundance of their globular clusters,

<sup>1</sup> The Macciò et al. (2008) c-M relation was used, giving up to 30% lower concentration than the Planck one used here, allowing a fit into a larger halo.

\* E-mail: arianna.dicintio@dark-cosmology.dk

Beasley et al. (2016) inferred a  $M_{\text{halo}}$  of  $(8\pm 4)\times 10^{10}M_{\odot}$  for VCC 1287, while Peng & Lim (2016) and Beasley & Trujillo (2016) determined a total mass of  $(\sim 9\pm 2)\times 10^{10}M_{\odot}$  for DF17, favouring the idea that UDGs are dwarfs. Further, Roman & Trujillo (2016) showed that the spatial distribution of UDGs in Abell 168 is compatible with the one of standard dwarfs.

A key question is whether UDGs can arise within a  $\Lambda$ CDM universe. An appealing possibility is that the formation of UDGs is not connected to the cluster environment, but rather to internal processes, such that UDGs already have a spatially extended stellar component when infalling into a cluster. Previous simulation works extensively showed that feedback driven gas outflows are able to cause expansion not only of the central DM distribution in galaxies (e.g. Governato et al. 2010; Di Cintio et al. 2014a,b; Oñorbe et al. 2015; Tollet et al. 2016; Chan et al. 2015; Read et al. 2016), but also of the stellar one (e.g. Teyssier et al. 2013; El-Badry et al. 2016; Dutton et al. 2016). The formation of DM density cores is related to rapid oscillation of the central potential driven by gas outflows following bursty star formation (e.g. Read & Gilmore 2005; Mashchenko et al. 2008; Pontzen & Governato 2012) and has been applied to observations to reconcile the *cusp-core* discrepancy (Katz et al. 2016). Interestingly, the mass range where we expect maximum efficiency in core formation overlaps with that of UDGs, i.e. galaxies with  $M^*\sim 10^{7-9}M_{\odot}$  should form large DM and stellar cores, while at higher and lower masses energy from stellar feedback alone becomes less efficient at creating cores (Di Cintio et al. 2014a,b; Dutton et al. 2016). It is thus natural to explore whether feedback driven expansion is a viable mechanism for the formation of UDGs. In this *Letter* we show that isolated UDGs, with a spatially extended stellar distribution, form naturally in dwarf-sized haloes by gas outflows. In Section 2 we introduce the hydrodynamical cosmological simulations used, in Section 3 we investigate the formation scenario of UDGs and show results focusing on global properties and gas content of UDGs, and in Section 4 we conclude by highlighting some observational predictions of our model.

## 2 SIMULATIONS

The simulated galaxies are taken from the Numerical Investigation of a Hundred Astrophysical Objects (NIHAO) project (Wang et al. 2015), evolved using the SPH code Gasoline (Wadsley et al. 2004; Keller et al. 2014). The code includes a subgrid model for turbulent mixing of metals and energy (Wadsley et al. 2008), ultraviolet heating, ionization and metal cooling (Shen et al. 2010). Star formation and feedback follows the model used in the MaGICC simulations (Stinson et al. 2013), that for the first time reproduced several galaxy scaling relations over a wide mass range (Brook et al. 2012), adopting a threshold for star formation of  $n_{\text{th}} > 10.3\text{cm}^{-3}$ .

Stars feed energy back into the ISM via blast-wave supernova feedback (Stinson et al. 2006) and early stellar feedback from massive stars. Particle masses and force softenings are chosen to resolve the mass profile to below 1% of the virial radius at all masses, ensuring that galaxy half-light radii are well resolved. The NIHAO galaxies cover a broad mass range, from dwarfs to Milky Way mass, and represent an unbiased sampling of merger histories, concentrations and spin parameters. The galaxies are all centrals and isolated, and lie on abundance matching predictions, having the expected  $M^*$  for each  $M_{\text{halo}}$ . The NIHAO project satisfactorily reproduces realistic galaxies in terms of their  $M^*$ , SFH, metals and DM distribution (e.g. Tollet et al. 2016; Obreja et al. 2016).

The haloes are identified using the AHF halo finder (Knollmann & Knebe 2009) and partially analysed with the *pybody* package (Pontzen et al. 2013).

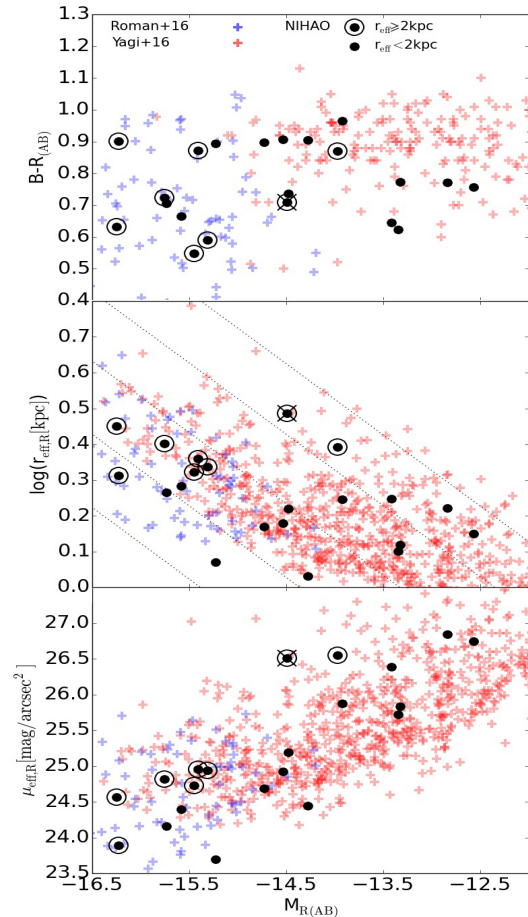


**Figure 1.** From top to bottom, we show  $B-R$ ,  $r_e$  and  $\mu_e$  as a function of  $R$ -band absolute magnitude of Coma cluster UDGs from Yagi et al. (2016) (red crosses) and of Abell 168 cluster and field UDGs from Roman & Trujillo (2016) (blue crosses). Diagonal lines represent constant  $\mu_e$  lines. Simulated UDGs with effective radii  $1 < r_e/\text{kpc} < 2$  are shown as black points, with extreme cases,  $r_e \geq 2$  kpc, further circled. The crossed UDG is analysed in Section 3.2 and Fig. 3.

## 3 RESULTS

Simulated galaxies are defined as UDGs if they satisfy the following criteria: i) their 2D effective radius,  $r_e$ , is larger than 1 kpc, ii) their absolute magnitude in  $R$  band is  $-16.5 \lesssim M_R \lesssim -12$ , corresponding to a stellar mass of  $10^7 \lesssim M^*/M_{\odot} \lesssim 10^{8.5}$ , iii) their effective surface brightness is low, with  $\mu_e > 23.5$  mag/arcsec $^2$ . It is worth noticing that several of the NIHAO galaxies fall in the UDGs category. To facilitate comparisons with observational results, we work in the AB system and used UBV $R_cI_c$  Johnson-Cousins filters. Galaxies are face-on (aligned via angular momentum of the stars) when computing  $r_e$  and the effective surface brightness is defined as  $L/(2\pi r_e^2)$  before converting it in units of mag/arcsec $^2$ .

A sample of 21 NIHAO simulations meet these requirements, shown in Fig. 1 as black points, with the largest-sized UDGs ( $r_e \geq 2$  kpc) further circled. One of the most extreme UDGs, with the largest  $r_e$  amongst the lowest surface brightness objects, is marked with a cross in Fig. 1 and it will be analysed in Section 3.2. In Fig. 1 we compare simulations with observed UDGs. From top to bottom the color  $B-R$ , the 2D effective radius and the effective surface brightness are shown against the absolute magnitude  $M_R$ .

$X$	$\bar{X} \pm \sigma$	$X_{min,max}$
$\log(M^* [M_\odot])$	$7.66 \pm 0.42$	6.83, 8.40
$\log(M_{halo} [M_\odot])$	$10.53 \pm 0.18$	10.22, 10.85
$\log(M_{HI} [M_\odot])$	$8.37 \pm 0.59$	7.22, 9.24
$r_e$ [kpc]	$1.87 \pm 0.53$	1.07, 3.06
$\mu_e$ [mag/arcsec <sup>2</sup> ]	$25.23 \pm 0.94$	23.69, 26.84
$M_R$	$-14.61 \pm 1.07$	-16.25, -12.57
B-R	$0.77 \pm 0.12$	0.54, 0.97
$n_{Sersic}$	$0.83 \pm 0.27$	0.31, 1.46
$\gamma(1-2\%R_{vir})$	$-0.37 \pm 0.18$	-0.78, -0.01
$\log(\lambda)$	$-1.48 \pm 0.25$	-2.04, -1.17
$c_{DM}$	$10.67 \pm 3.05$	5.89, 18.85

**Table 1.** Average properties of the simulated UDG sample. Concentrations and spin parameters have been computed in the original DM-only run.

SDSS *gri* colors and magnitudes used in Roman & Trujillo (2016) were converted to BR Subaru-Suprime-Cam ones used in Yagi et al. (2016) by adopting the color conversions derived in the appendix of Yoshida et al. (2016). When comparing  $r_e$  and  $\mu_e$  with the Roman & Trujillo (2016) data we used their r-band results, as best approximation of our R-band ones.

Simulated UDGs overlap with observational data in color, effective radii, surface brightness and magnitude. While most of the Coma cluster UDGs follow the red sequence with B-R=0.8-1.2, the Abell 168 region, including both cluster and field UDGs, span a wider range in colors, with the bluest objects having B-R~0.4. This broad range in colors is also observed in the simulated UDGs, some of which have recent star formation (see Section 3.3), an indication that not all UDGs are evolving passively and suggesting that the isolated counterparts of cluster UDGs may not be quenched.

### 3.1 UDGs: global properties of the simulated sample

In Table 1 we summarize the properties of simulated UDGs: from top to bottom we specify stellar mass, halo mass, HI gas mass ( $M_{HI}$ ), 2D effective radius, effective surface brightness, R-band absolute magnitude, B-R color, Sérsic index, DM halo inner slope, spin parameter and concentration. Specifically, the Sérsic index  $n_{Sersic}$  is computed by fitting the 2D surface brightness profile in R-band out to  $2 \times r_e$  with a Sérsic profile (Sersic 1968), the inner slope  $\gamma$  of the DM halo is found by fitting its density profile with a power law between 1 and 2% of the virial radius, in a region where all our galaxies are well resolved, the dimensionless spin parameter  $\lambda$  follows the Bullock et al. (2001) definition and the concentration  $c$  is computed from the original DM-only simulation.

All the currently observed structural properties of UDGs ( $M^*$ ,  $n_{Sersic}$ , color,  $M_R$ ,  $r_e$  and  $\mu_e$ ) are in excellent agreement with the ones of the simulated sample. The mean value of the spin parameter is close to the peak of the distribution of spin parameters for DM haloes ( $\log(\lambda) \sim -1.45$ , Bullock et al. 2001), indicating that our simulated UDGs do not live in particularly high-spin objects as suggested by Amorisco & Loeb (2016). The range of DM inner slopes,  $-0.78 < \gamma < -0.01$ , shows that UDGs live in expanded DM haloes, whose logarithmic inner slope is shallower than the universal NFW value of  $\gamma = -1$ . We will see in Section 3.2 how this is closely linked to the formation of UDGs.

Interestingly, the simulated UDGs have a non-negligible amount of HI gas, whose fraction at  $z=0$  is computed including self-shielding and ionization from star forming regions as in Gutcke et al. (2016). While most recent observations focused on UDGs

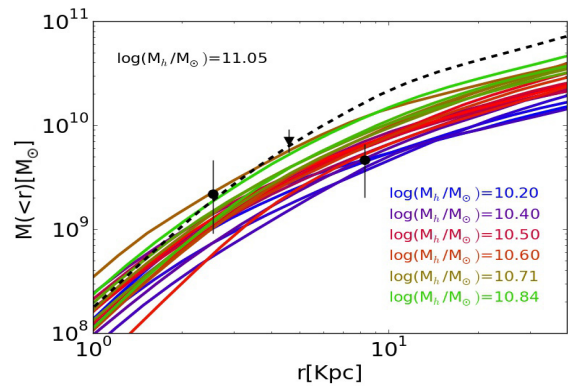


**Figure 2.** Mass profiles of simulated UDGs, color coded by DM halo mass, including contributions from DM, gas and stars. Overplotted observational results from Beasley et al. (2016), VCC 1287 UDG as circles points, and from van Dokkum et al. (2016), DF 44 UDG as triangle.

in clusters, finding the not surprising result that those objects are gas-poor, there is no current evidence that isolated UDGs should be gas-poor: indeed, the only work that focused on isolated UDGs could only place an upper limit of  $M_{HI} < 10^{8.8} M_\odot$  on the expected amount of HI gas in DGSAT I (Martínez-Delgado et al. 2016), suggesting that values of  $7 \lesssim \log_{10}(M_{HI}/M_\odot) \lesssim 9$ , as predicted by our simulations, are fully within observational constraints. Note that the  $M_{HI}$  amount that UDGs should have once falling into a cluster can not be inferred by using our isolated simulations.

Remarkably, the simulated UDGs have average halo mass  $M_{halo} = 10^{10.53} M_\odot$  and a maximum and minimum  $M_{halo}$  of  $10^{10.22}$  and  $10^{10.85} M_\odot$ , respectively: they are therefore legitimate dwarfs rather than failed  $L^*$  objects. Such dwarf halo mass range is also advocated in Amorisco & Loeb (2016), although their model requires high halo spin, unlike what we see in our simulated UDGs.

The halo masses of the simulated galaxies are in agreement with the inferred mass of UDGs in the Virgo (Beasley et al. 2016) and Coma clusters (Peng & Lim 2016; Beasley & Trujillo 2016). We plot in Fig. 2 their total mass profiles together with the two available measurements of the mass of VCC 1287 (circles), obtaining a halo mass between  $10.20 < \log_{10}(M_{halo}/M_\odot) < 10.80$ , in agreement with estimates from Beasley et al. (2016). We also show DF 44 UDG (triangle) as in van Dokkum et al. (2016), who inferred a  $\sim 8 \times 10^{11} M_\odot$  halo mass for this galaxy: we show here that a  $M_{halo} = 10^{11.05} M_\odot$  matches this observation, by plotting as dashed line the mass profile of a simulated UDG with a similar  $M^*$  as DF 44 and effective radius of 4.4 kpc (not shown in Fig. 1 due to magnitude cut), corroborating the finding that even the brightest UDGs are not Milky-Way mass objects.

Finally, the concentrations of simulated UDGs are typical of galaxies of their halo masses, excluding the possibility that UDGs form in haloes with  $c$  systematically higher or lower than average.

### 3.2 UDGs: formation scenario

We analyse the properties of the UDG marked with a cross in Fig. 1 to show how such objects can form. In Fig. 3 we show, a) a visualization of the stellar distribution at  $z=0$  using a 3-color image based on IVU bands, b) the star formation history (SFH) of the galaxy, c) the evolution of the 3D stellar density as a function of redshift for all stars (solid lines) and old stars ( $t_{form} < 5$  Gyrs, dashed lines) and d) the evolution of DM density, logarithmic inner slope  $\gamma$  and total amount of mass  $m_1 = \log_{10}(M_{<1kpc}/M_\odot)$  contained within 1 kpc

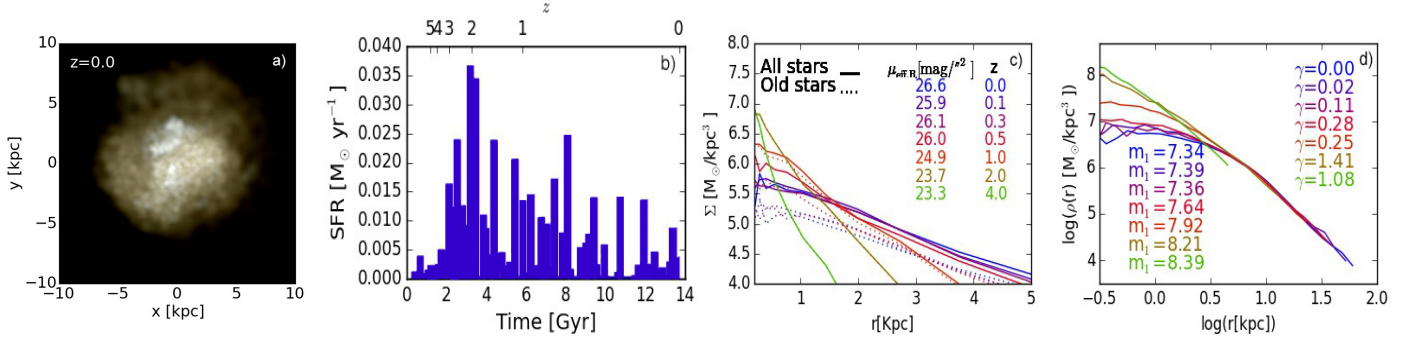


**Figure 3.** Formation of the UDG marked with a cross in Fig.1. From left to right: a) face-on multi-band image of stars at  $z=0$ , b) SFH, c) 3D spherically averaged stellar density profile color coded by  $z$  and d) evolution of DM density profile. Panel c): the contribution of all stars and old stars formed within the first 5 Gyrs of the galaxy’s life is indicated as solid and dashed line, respectively; the  $\mu_e$  evolution is shown as well. Panel d): the DM density inner slope measured within 1 and 2% of the galaxy virial radius and the total enclosed mass at 1 kpc ( $m_1 = \log_{10}(M_{<1\text{kpc}}/M_{\odot})$ ) are indicated as a function of  $z$ .

of the galaxy as a function of redshift. The bursty SFH of the UDG can be appreciated in panel b), including peaks in the last Gyr of its history, indicating recent episodes of star formation: this feature is also reflected in the blue off-centered over-density visible in the colour image of panel a), similar to DGSAT I UDG observed in [Martínez-Delgado et al. \(2016\)](#).

The formation scenario of UDGs is illustrated in panels c) and d): as the DM halo expands and forms a central core due to episodic and powerful gas outflows driven by star formation, the stellar distribution expands as well. In panel c) the effective surface brightness is shown as a function of redshift: as  $r_e$  increases,  $\mu_e$  decreases bringing the dwarf onto the UDG regime. This galaxy became an ultra diffuse one by  $z=1.5$ . To confirm that  $r_e$  increases due to expansion of the stellar distribution rather than by new episodes of star formation in the outer regions, we separate the contribution of all stars and old stars: we observe that even the oldest stellar population expands as a response to the core creation mechanism. A spatially extended stellar distribution, typical of UDGs, can therefore arise from internal feedback processes, which also give rise to a spherical rather than disk galaxy. An extensive study of UDGs morphologies will be presented in forthcoming work.

### 3.3 UDGs: gas content and star formation history

We investigate what makes UDGs differ from more compact galaxies in the same stellar mass range. In Fig. 4 we show the SFH of six galaxies whose effective radii are the largest (right column) and smallest (left column) in their respective mass bin. Fig. 4 therefore includes both UDGs as well as more compact, regular dwarfs. From top to bottom, we pair galaxies with similar halo and stellar masses, quoting in each panel the  $r_e$ ,  $M_R$ ,  $M^*$ ,  $M_{\text{HI}}$ , extension of HI gas ( $R_{\text{HI}}$ , as the radius at which the HI surface density reaches  $1 M_{\odot}/\text{pc}^2$ ) and baryon fraction relative to the cosmic one,  $f_{b,c}$ .

The difference in properties between the most extreme UDGs (right panels) and the less extreme, more compact dwarfs (left panels) are striking. Galaxies with large  $r_e$  also have a larger  $M_{\text{HI}}$ , baryon fraction and  $R_{\text{HI}}$ , and more prolonged and persistently bursty SFH, including a larger fraction of young stellar population, compared to galaxies with a smaller  $r_e$ . When most of star formation happens in the first  $\sim 3$ -4 Gyrs, feedback can eject significant amounts of gas from relatively shallow potential wells at early times (e.g. [Dekel & Silk 1986](#)), resulting in low baryon fractions by  $z=0$ . Since gas is expelled at early stages, there is less gas

for ongoing star formation and crucially there is less gas to be expelled from the inner regions when star formation occurs, being this the key aspect of the mechanism for core creation: the lower is the gas fraction at a given epoch, the less efficient is such mechanism. We verified that the dwarfs with lower  $r_e$  have retained at most 10% of the initial gas mass between  $z=4$  and 1, while the largest  $r_e$  UDGs have kept up to 50% of the initial gas within the same period. The less expanded galaxies have a very low baryon fraction,  $f_b/f_{b,c} \sim 6$ -13% by  $z=0$ , and retain up to two order of magnitudes less HI gas than similar  $M^*$  galaxies with larger  $r_e$ ; their DM inner slope is less shallow and correspondingly the distribution of HI is more compact, with  $R_{\text{HI}} \sim 0.9$ -1.6 kpc.

Oppositely, galaxies with star bursts occurring after the rapid halo growth phase has finished are the ones that can keep their gas, which can not escape the deeper potential well: they have enough gas available at all time to drive DM cores and a spatially extended stellar distribution, retaining about 50%  $f_{b,c}$  and up to  $10^9 M_{\odot}$  in HI gas by  $z=0$ . A similar dependence of core sizes with SFH has been found in [Oñorbe et al. \(2015\)](#) and [Read et al. \(2016\)](#) for lower mass objects than the ones studied here, with  $M_{\text{halo}} \sim 10^{7-10} M_{\odot}$ .

We conclude by summarizing the differences between regular dwarfs (such as the top-left galaxy in Fig. 4) and UDGs within a similar  $M^*$  range: non-UDGs have smaller effective radius, less gas mass and baryon fraction, steeper DM inner slope and a higher Sérsic index than UDGs, while their halo mass, color, magnitude, spin parameter and concentration are indistinguishable from the ones of UDGs. This further validates the finding that the availability of gas is crucial to the formation mechanism of UDGs.

## 4 CONCLUSIONS

We showed that cosmological simulations of isolated galaxies from the NIHAO project, which include feedback from SNe and massive stars, reproduce a population of Ultra-Diffuse Galaxies (UDGs) with stellar mass, magnitude, colour, Sérsic index, effective radius and surface brightness in agreement with observations. Internal processes, rather than environmental ones, are at the base of the formation scenario of UDGs. Feedback driven gas outflows give rise to a spatially extended stellar component, while simultaneously expanding the dark matter halo, leading to the emergence of low surface brightness dwarf galaxies, or UDGs, with  $M^* \sim 10^{7-9} M_{\odot}$  and  $r_e \sim 1$ -3 kpc. A key aspect is the availability of gas that is driven away from central regions during bursts of star formation, causing

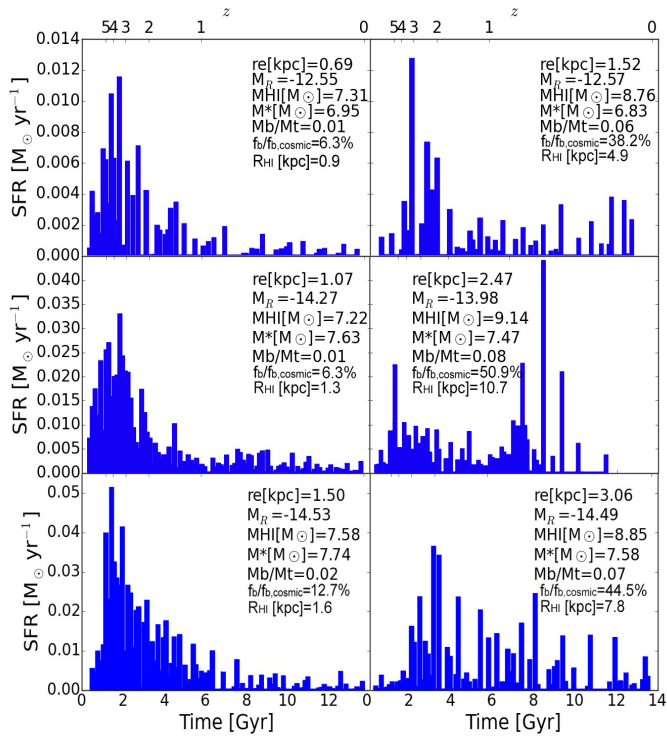


**Figure 4.** SFHs of galaxies with the largest (right column) and smallest (left column) effective radius in their mass bin. From top to bottom, each row shows galaxies with similar halo mass and magnitude,  $\log_{10}(M_{\text{halo}}/M_{\odot}) \sim 10.20, 10.45, 10.50$  and  $M_R \sim -12.5, -14.0, -14.5$ . In each panel  $r_e$ ,  $M_R$ ,  $M_{\text{HI}}$ ,  $M^*$ ,  $f_b$  and HI radius are indicated.

rapid oscillations of the potential: galaxies that expel most of their gas at early times are less efficient at causing expansion than galaxies of similar  $M^*$  that retain more gas for later times. Our findings imply that UDGs:

- are dwarf galaxies, with  $10^{10} \lesssim M_{\text{halo}}/M_{\odot} \lesssim 10^{11}$ , in agreement with mass estimates from Beasley et al. (2016), Beasley & Trujillo (2016) and Peng & Lim (2016), and with our revised mass estimate of the van Dokkum et al. (2016) DF 44 UDG: they naturally extend the population of LSB galaxies to the dwarf regime;
- are not exclusively associated to a cluster environment: they are expected to be found in the field as well;
- are not all red and quenched: we found simulated UDGs with  $B-R < 0.7$  and recent off-centered star formation, as well as UDGs with  $B-R > 0.7$  that only stopped forming stars in the past 2 Gyrs;
- have typical distributions of halo spin and concentration, an average Sérsic index of less than one and dark-matter cores;
- if isolated, have significant HI gas mass,  $M_{\text{HI}} \sim 10^{7-9} M_{\odot}$ : at a similar stellar mass, the larger the effective radius, the higher is the baryon fraction retained within the virial radius and the larger is the amount and extent of HI gas, with  $R_{\text{HI}}$  up to  $\sim 10.7$  kpc; moreover, the larger  $r_e$ , the higher is the fraction of young stellar population expected in isolated UDGs.

The first three points of the list are in common with the model of Amorisco & Loeb (2016) although, unlike our scenario, those authors appealed to high spin haloes in order to form UDGs.

Given their predicted  $M_{\text{HI}}$ , some UDGs should be seen, or have already been seen, by the HI Alfralfa survey (Giovanelli et al. 2005; Haynes et al. 2011). Indeed, some *dark galaxies* in Alfralfa,

those without a clear optical counterpart, have only recently been identified with LSB objects (Cannon et al. 2015) and have HI mass  $7.4 < \log(M_{\text{HI}}/M_{\odot}) < 9.5$ . Deep optical imaging (Janowiecki et al. 2015) shows that the system HI1232+20 has magnitude, HI mass, surface brightness, colors and remarkably a large  $R_{\text{HI}}$  (5.1 to 11.2 kpc) in agreement with our most expanded UDGs. The fraction of *dark galaxies* over the total number of detected HI sources, within a completeness radius of 20 Mpc and having the expected  $M_{\text{HI}}$  mass of UDGs, is as high as 8.5% in the Alfralfa  $\alpha.70$  catalogue: some of them may be UDGs, and future dedicated observations can help verify our claim. Finally, in the SPARC sample of local HI-rich galaxies (Lelli et al. 2016), 70% of the galaxies with  $10^7 < M^*/M_{\odot} < 10^{8.5}$  have  $r_e > 1$  kpc whilst 20% have  $r_e > 2$  kpc, giving surface brightnesses in the realm of UDGs, and showing that such sizes are not rare amongst dwarfs after all.

We proposed a scenario in which UDGs form naturally by outflow episodes in haloes of  $M_{\text{halo}} \sim 10^{10-11} M_{\odot}$ , in the same mass range where feedback induced expansion is expected to be most efficient at creating a cored distribution of DM and stars (e.g. Di Cintio et al. 2014a; Tollet et al. 2016; Dutton et al. 2016): the existence of a preferential halo mass for UDGs therefore fits within our theoretical understanding of how stellar feedback impacts the DM and stellar distribution in galaxies. This picture agrees with models in which the effect of repeated outflows accumulates during cosmic time (e.g. Read & Gilmore 2005; Pontzen & Governato 2012; Dutton et al. 2016): we demonstrate here for the first time that it is the gas availability that drives both the SFH and the amount of expansion of DM and stars, with higher gas fractions more efficiently expanding both the stellar and DM component, leading to the emergence of low surface brightness, gas-rich, HI extended, UDGs.

Larger diffuse galaxies, with  $r_e$  up to 7-8 kpc, exist as well in the NIHAO simulations, with  $M^*$  higher than the presently observed UDGs: they can be classified as regular LSBs and will be the subject of a future paper (Di Cintio in prep).

## ACKNOWLEDGEMENTS

The authors kindly thank M. Yagi, J. Koda, I. Trujillo, J. Roman, M. Beasley, E. Papastergis, M. Haynes, F. Lelli and N. Amorisco for sharing their data and for fruitful discussions. Computational resources were provided by the High Performance Computing at NYUAD, the THEO cluster at MPIA and the HYDRA clusters at Rechenzentrum in Garching. ADC thanks the Carlsberg foundation. CBB thanks MINECO/FEDER grant AYA2015-63810-P. AD is supported by grants ISF 124/12, BSF 2014-273.

## REFERENCES

- Amorisco N. C., Loeb A., 2016, *MNRAS*, **459**, L51  
 Beasley M. A., Trujillo I., 2016, preprint, (arXiv:1604.08024)  
 Beasley M. A., Romanowsky A. J., Pota V., Navarro I. M., Martinez Delgado D., Neyer F., Deich A. L., 2016, *ApJ*, **819**, L20  
 Brook C. B., Stinson G., Gibson B. K., Wadsley J., Quinn T., 2012, *MNRAS*, **424**, 1275  
 Bullock J. S., Dekel A., Kolatt T. S., Kravtsov A. V., Klypin A. A., Porciani C., Primack J. R., 2001, *ApJ*, **555**, 240  
 Cannon J. M., et al., 2015, *AJ*, **149**, 72  
 Chan T. K., Kereš D., Oñorbe J., Hopkins P. F., Muratov A. L., Faucher-Giguère C.-A., Quataert E., 2015, *MNRAS*, **454**, 2981  
 Dekel A., Silk J., 1986, *ApJ*, **303**, 39  
 Di Cintio A., Brook C. B., Macciò A. V., Stinson G. S., Knebe A., Dutton A. A., Wadsley J., 2014a, *MNRAS*, **437**, 415  
 Di Cintio A., Brook C. B., Dutton A. A., Macciò A. V., Stinson G. S., Knebe A., 2014b, *MNRAS*, **441**, 2986

- Dutton A. A., et al., 2016, *MNRAS*, **461**, 2658
- El-Badry K., Wetzel A., Geha M., Hopkins P. F., Kereš D., Chan T. K., Faucher-Giguère C.-A., 2016, *ApJ*, **820**, 131
- Giovanelli R., et al., 2005, *AJ*, **130**, 2598
- Governato F., et al., 2010, *Nature*, **463**, 203
- Gutcke T. A., Stinson G. S., Macciò A. V., Wang L., Dutton A. A., 2016, *MNRAS*,
- Haynes M. P., et al., 2011, *AJ*, **142**, 170
- Impey C., Bothun G., 1997, *ARA&A*, **35**, 267
- Janowiecki S., et al., 2015, *ApJ*, **801**, 96
- Katz H., Lelli F., McGaugh S. S., Di Cintio A., Brook C. B., Schombert J. M., 2016, preprint, ([arXiv:1605.05971](https://arxiv.org/abs/1605.05971))
- Keller B. W., Wadsley J., Benincasa S. M., Couchman H. M. P., 2014, *MNRAS*, **442**, 3013
- Knollmann S. R., Knebe A., 2009, *ApJS*, **182**, 608
- Koda J., Yagi M., Yamanoi H., Komiyama Y., 2015, *ApJ*, **807**, L2
- Lelli F., McGaugh S. S., Schombert J. M., 2016, preprint, ([arXiv:1606.09251](https://arxiv.org/abs/1606.09251))
- Macciò A. V., Dutton A. A., van den Bosch F. C., 2008, *MNRAS*, **391**, 1940
- Martínez-Delgado D., et al., 2016, *AJ*, **151**, 96
- Mashchenko S., Wadsley J., Couchman H. M. P., 2008, *Science*, **319**, 174
- McGaugh S. S., Schombert J. M., Bothun G. D., 1995, *AJ*, **109**, 2019
- Mihos J. C., et al., 2015, *ApJ*, **809**, L21
- Muñoz R. P., et al., 2015, *ApJ*, **813**, L15
- Oñorbe J., Boylan-Kolchin M., Bullock J. S., Hopkins P. F., Kereš D., Faucher-Giguère C.-A., Quataert E., Murray N., 2015, *MNRAS*, **454**, 2092
- Obreja A., Stinson G. S., Dutton A. A., Macciò A. V., Wang L., Kang X., 2016, *MNRAS*, **459**, 467
- Peng E. W., Lim S., 2016, *ApJ*, **822**, L31
- Pontzen A., Governato F., 2012, *MNRAS*, **421**, 3464
- Pontzen A., Roškar R., Stinson G., Woods R., 2013, pynbody: N-Body/SPH analysis for python, Astrophysics Source Code Library ([ascl:1305.002](https://ascl.net/1305.002))
- Read J. I., Gilmore G., 2005, *MNRAS*, **356**, 107
- Read J. I., Agertz O., Collins M. L. M., 2016, *MNRAS*, **459**, 2573
- Roman J., Trujillo I., 2016, preprint, ([arXiv:1603.03494](https://arxiv.org/abs/1603.03494))
- Sandage A., Binggeli B., 1984, *AJ*, **89**, 919
- Schombert J., Maciel T., McGaugh S., 2011, *Advances in Astronomy*, **2011**, 143698
- Sersic J. L., 1968, Atlas de galaxias australes
- Shen S., Wadsley J., Stinson G., 2010, *MNRAS*, **407**, 1581
- Stinson G., Seth A., Katz N., Wadsley J., Governato F., Quinn T., 2006, *MNRAS*, **373**, 1074
- Stinson G. S., Brook C., Macciò A. V., Wadsley J., Quinn T. R., Couchman H. M. P., 2013, *MNRAS*, **428**, 129
- Teyssier R., Pontzen A., Dubois Y., Read J. I., 2013, *MNRAS*, **429**, 3068
- Töllet E., et al., 2016, *MNRAS*, **456**, 3542
- Wadsley J. W., Stadel J., Quinn T., 2004, *NewA*, **9**, 137
- Wadsley J. W., Veeravalli G., Couchman H. M. P., 2008, *MNRAS*, **387**, 427
- Wang L., Dutton A. A., Stinson G. S., Macciò A. V., Penzo C., Kang X., Keller B. W., Wadsley J., 2015, *MNRAS*, **454**, 83
- Yagi M., Koda J., Komiyama Y., Yamanoi H., 2016, *ApJS*, **225**, 11
- Yoshida M., Yagi M., Ohyama Y., Komiyama Y., Kashikawa N., Tanaka H., Okamura S., 2016, *ApJ*, **820**, 48
- Yozin C., Bekki K., 2015, *MNRAS*, **452**, 937
- van Dokkum P. G., Abraham R., Merritt A., Zhang J., Geha M., Conroy C., 2015a, *ApJ*, **798**, L45
- van Dokkum P. G., et al., 2015b, *ApJ*, **804**, L26
- van Dokkum P., et al., 2016, *ApJ*, **828**, L6
- van der Burg R. F. J., Muzzin A., Hoekstra H., 2016, *A&A*, **590**, A20